Fluorescence and Absorption Properties of Perylenyl and Perylenoyl Probe Molecules in Solvents and Liquid Crystals

Lennart B.-Å. Johansson,* Julian G. Molotkovsky, and Lev D. Bergelson

Contribution from the Department of Physical Chemistry, University of Umeå, S-901 87 Umeå, Sweden, and M. M. Shemyakin Institute of Bioorganic Chemistry, U.S.S.R. Academy of Sciences, Miklukho-Maklaya 16/10 117988, Moscow, U.S.S.R. *Received April 23, 1987*

Abstract: Light spectroscopic properties of fluorescent derivatives of perylene in solvents and lyotropic liquid crystals have been investigated. These were 2,5,8,11-tetra-*tert*-butylperylene, methyl 4-(3-perylenyl)butyrate, methyl 3-(3-perylenoyl)propionate, 3-(3-perylenoyl)propionic acid, 9-(3-perylenoyl)nonanoic acid, and *N*-[9-(3-perylenoyl)nonanoyl]sphingosine-1-phosphocholine. The first two compounds are hereafter referred to as perylenyls, while the latter four are named perylenoyls. Absorption and fluorescence spectra and fluorescence lifetimes of the perylenyls are found to be very similar to those of perylene. Both absorption and fluorescence spectra of the perylenoyls are broadened and red-shifted compared to those of perylene. The fluorescence spectrum is strongly red-shifted with increasing solvent polarity, which is not the case for the perylenyls. Photophysical data of the perylenyl and the perylenoyl molecules in various solvents, micelles, and liquid crystals are given. It is shown that the absorption and fluorescence dipole moments for the $S_0 \leftrightarrow S_1$ transitions are parallel in both kinds of chromophores. The orientation of these probe molecules in a macroscopically aligned liquid crystal has been obtained from linear dichroism measurements and time-resolved fluorescence anisotropy. It is concluded that the orientation of a probe in its electronic ground state may differ from that in the excited state. Information about rotational motions of the different fluorophores solubilized in micelles and liquid crystals was obtained from the fluorescence anisotropy. The fluorescent moiety of the probe undergoes rotational motions *locally* in the amphiphile aggregate which are typically about 1-3 ns. A slower correlation time ranging from 10 to 40 ns is ascribed to translational diffusion of the fluorophore in the aggregate.

Fluorescent molecules are frequently used as probes in studies of (bio)polymers,[1] lipid membranes,[2] the physical properties of energy,[3] and electron-transfer processes.[4] A large number of fluorophores are available, but in practice few fulfill all the basic criteria needed in solving a particular problem. For example, 1,6-diphenyl-1,3,5-hexatriene (DPH), which is probably the most popular probe in lipid research, is photobleached by UV radiation and has a very complex photophysics.[5,6] Recently, it was also shown[7,8] that DPH reorients upon electronic excitation or might fluoresce with a transition dipole moment which is not parallel to the dipole moment of the strongly absorbing band at about 370 nm. Perylene is photostable, has a monoexponential decay of its photophysics,[9,10] and does not reorient in a lipid bilayer upon electronic excitation.[7] Therefore, derivatives of perylene, which recently have been synthesized,[11,12] might prove to be better suited as probes in membrane research. We here present an extensive study of spectral and photophysical properties of various perylene derivatives. These compounds are 2,5,8,11-tetra-*tert*-butylperylene, methyl 4-(3-perylenyl)butyrate, methyl 3-(3-perylenoyl)propionate, 3-(3-perylenoyl)propionic acid, 9-(3-perylenoyl)nonanoic acid, and *N*-[9-(3-perylenoyl)nonanoyl]sphingosine-1-phosphocholine. Light spectroscopic data on 2,5,8,11-tetra-*tert*-butylperylene and methyl 4-(3-perylenyl)butyrate have to our knowledge not been presented previously, while some spectral properties of the perylenoyl derivatives are available.[11,12]

The spectroscopic tools and the theoretical models necessary for interpreting the experimental results are briefly summarized in General Considerations, in this paper. The outline of Results and Discussion is as follows. First, the properties of absorption and fluorescence spectra in various solvents, micelles, and lyotropic liquid crystals are given. The fluorescence lifetimes in these media are then presented, with particular emphasis on the photophysical heterogeneity observed in micelles and liquid crystals. The next subsection deals with the polarizations of the absorption and emission transition dipole moments, which for all compounds are found to be parallel. These results are based on linear dichroism and fluorescence anisotropy experiments that also yield information about the ground- and excited-state orientational distributions of the various fluorophores in a macroscopically aligned liquid crystal. We finally present fluorescence anisotropy studies of some perylenyl and perylenoyl probes solubilized in micelles, a cubic lyotropic liquid crystalline phase, and a lyotropic nematic liquid crystal. These data provide information concerning the orientation and different motions of the probes in detergent aggregates.

Materials

Perylene (EGA-Chemie) was recrystallized three times from ethanol of spectroscopic grade. 2,5,8,11-Tetra-*tert*-butylperylene (TBPe) was synthesized at the Department of Organic Chemistry 2, University of Lund, Sweden. Perylene was Friedel-Crafts alkylated in *tert*-butyl chloride with $AlCl_3$. This mixture was reflux-boiled during one night. Next day *tert*-butyl chloride and $AlCl_3$ were added and then reflux-boiled for another 6 h. A saturated NaCl solution was added. The phases were then separated and the water phase twice extracted with CH_2Cl_2. The organic phases were mixed and washed with water and a saturated $NaHCO_3$ solution. The organic phase was dried (Na_2SO_4) and evaporated. The remainder was purified on silica gel column using heptane as the eluting solvent. The ^1H NMR chemical shifts are in excellent agreement with those previously reported.[13] The preparation was also checked by HPLC and no other components were found. The molar absorptivity (ϵ) of TBPe in ethanol was found to be 28×10^3 mol^{-1} dm^3 cm^{-1} at 435 nm (i.e., the vibronic peak of maximum intensity in the $S_0 \rightarrow S_1$ vibronic progression).

The syntheses of the perylenoyl probes are described elsewhere.[37] Briefly, perylene was Friedel-Crafts acylated with excess sebacic acid dichloride ($AlCl_3$, -6 to -4 °C, 30 min) in nitromethane. Then the mixture was treated with excess methanol (1 h at -20 °C, and 1 h at room temperature). The resulting methyl 9-(3-perylenoyl)nonanoate was separated by silica gel column chromatography using chloroform-toluene

(1) Vlovy, J. L.; Monnerie,; Brochon, J. C. *Macromolecules* **1983**, *16*, 1845 and references therein.
(2) Johansson, L. B.-Å.; Lindblom, G. *Q. R. Biophys.* **1980**, *13*, 63 and references therein.
(3) Domingue, R. P.; Fayer, M. D. *J. Phys. Chem.* **1986**, *80*, 5141.
(4) Ediger, M. D.; Fayer, M. D. *Int. Rev. Phys. Chem.* **1985**, *4*, 207.
(5) Hudson, B. S.; Kohler, B. E.; Schulten, K. In *Excited States*; Lim, E. C., Ed.; Academic Press: New York, 1982; Vol. 6.
(6) Mason, R.; Cehelnik, E. D. *J. Photochem.* **1978**, *9*, 219.
(7) Johansson, L. B.-Å. *Chem. Phys. Lett.* **1986**, *118*, 516.
(8) Mulders, F.; van Langen, H.; van Ginkel, G.; Levine, Y. K. *Biochim. Biophys. Acta* **1986**, *859*, 209.
(9) Barkley, M. D.; Kowalczyk, A. A.; Brand, L. *J. Chem. Phys.* **1981**, *75*, 3581.
(10) Christensen, R. L.; Drake, R. C.; Phillips, D. *J. Phys. Chem.* **1986**, *90*, 5960.
(11) Molotkovsky, J. G.; Manevich, Y. M.; Babak, V. I.; Bergelson, L. D. *Biochem. Biophys. Acta* **1984**, *778*, 281.
(12) Bergelson, L. D.; Molotkovsky, J. G.; Manevich, Y. M. *Chem. Phys. Lipids* **1985**, *37*, 165.
(13) Minsky, A.; Meyer, Y.; Rabinovitz, M. *J. Am. Chem. Soc.* **1982**, *104*, 2475.

0002-7863/87/1509-7374$01.50/0

mixtures as eluent. The above methyl ester was hydrolyzed in 2-propanol – 1 N NaOH, 5:2, v/v (70 °C, 1 h) to give 9-(3-perylenoyl)nonanoic acid, mp 194–196 °C (from chloroform).

3-(3-Perylenoyl)propionic acid was obtained by the Friedel–Crafts acylation of perylene with succinic acid dichloride in the above conditions (decomposition by HCl with ice; separation on silica gel column with chloroform–*i*-PrOH–AcOH, 95:4:1, v/v/v), mp 248–250 °C dec (ref 38: mp 255 °C). The acid was converted to the methyl ester by diazomethane in methylene chloride.

Both substances were obtained as orange powders and contained ca. 2–4% of inseparable admixtures, presumably positional isomers (HPCL data).

Sphingosine-1-phosphocholine[39] was acylated with 9-(3-perylenoyl)-nonanoic acid in the presence of dicyclohexylcarbodiimide and 4-dimethylaminopyridine in 2-propanol – chloroform – triethylamine (5:5:1 by volume, 1 day at room temperature). *N*-[9-(3-Perylenoyl)nonanoyl]-sphingosine-1-phosphocholine was purified by silica gel column chromatography with a chloroform – methanol gradient elution, and obtained as a chromatographically homogeneous red amorphous substance.

All perylenoyl derivatives revealed two main absorption maxima: 259 and 447 nm, with $\epsilon \approx 2.9 \times 10^4$ and 2.4×10^4, respectively (in ethanol).

4-(3-Perylenyl)butyric acid was a generous gift of Dr. T. A. Chibisova (D. I. Mendeleev Institute of Chimical Technology, Moscow). This substance was synthesized by the Huang-Minlon reduction of 3-(3-perylenoyl)propionic acid. Methyl 4-(3-perylenyl)butyrate was obtained from the acid by treatment with diazomethane.

Ethanol (99.5%, spectroscopic grade), 1,2-propanediol (Merck, proanalysi), and glycerol (Omnisolv, BDH, spectroscopic grade) were all used as received after checking the fluorescence background. 1,4-Dioxane (Aldrich-Chemie; spectroscopic grade) and acetonitrile (Merck, pro analysi) were dried by using Na. Methanol (Merck, spectroscopic grade) and deuterated (CH_3OD) methanol (Ciba-Geigy, Switzerland) were used as received. Olive oil (Sigma) was dissolved in a suspension of charcoal and hexane. The suspension was stirred and filtered. Charcoal was added to the filtered solution and again stirred and filtered. Hexane was then evaporated.

The lyotropic nematic liquid crystalline phase (LNLC) was composed of potassium dodecanoate (laurate)/KCl/and D_2O in the amounts 34.00/2.30/63.70 % by weight. Potassium laurate was synthesized and purified as described in ref 14 and 32 where also a detailed description of the sample preparation is given. The LNLC phase was kept in a fluorescence cuvette (10 × 10 mm optical path lengths) and macroscopically aligned in a magnetic field of 5.9 T for about 12 h. Pentaethyleneglycol mono-*n*-dodecyl ether ($C_{12}EO_5$) was purchased from Nikko Chemicals Ltd. (Tokyo, Japan) and used as received. The micellar and the cubic liquid crystalline phases were composed of $C_{12}EO_5$ and water in the amounts 25.0:75.0 and 65.0:35.0 wt %, respectively.

Methods

The time-resolved single photon counting experiments were monitored on a PRA System 3000 (Photophysical Research Associates, Canada). The excitation source was a thyratron-gated flash lamp (Model 510 C) filled with D_2 and operating at ~30 kHz. The excitation and emission wavelengths were selected by interference filters (Omega/Saven AB, Sweden) centered at 359.8 nm (HBW = 10.1 nm), 398.8 (11.4), 409.4 (13.0), 430.0 (10.0), 447.8 (27.6), 477.0 (11.4), 500.0 (12.1), 520.0 (12.3), 545.0 (28.2), and 550.9 (9.4). The polarized fluorescence decay curves were measured by repeated collection of data during typically 120 s, for each setting of the polarizers. The excitation polarizer was fixed and the emission polarizer periodically rotated. In each experiment the decay curves $F_{zz}(t)$ and $F_{zx}(t)$ (c.f. General Considerations) were collected. From these a sum curve

$$S(t) = F_{zz}(t) + 2GF_{zx}(t)$$

and a difference curve

$$D(t) = F_{zz}(t) - GF_{zx}(t)$$

were calculated. The correction factor, G, was obtained by normalizing the total number of counts F_{zz} and F_{zx} collected in $F_{zz}(t)$ and $F_{zx}(t)$, respectively, to the average value of the steady-state emission anisotropy, r_s as

$$G = [(1 - r_s)/(1 + 2r_s)]F_{zz}/F_{zx}$$

(14) Johansson, L. B.-Å.; Lindblom, G. *Liq. Cryst.* **1986**, *1*, 53.

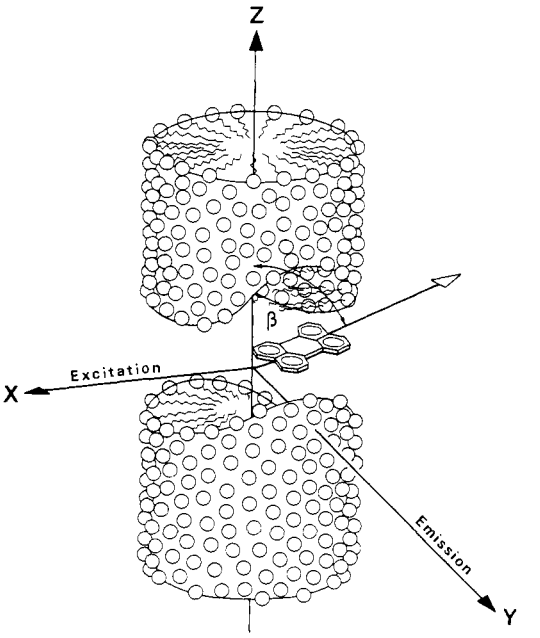

Figure 1. A schematic picture of a macroscopically aligned amphiphile aggregate. The C_∞ symmetry axis of the aggregate coincides with the optical axis and the Z axis of a laboratory fixed coordinate system. The $S_0 \rightarrow S_1$ electronic transition dipole moment of a solubilized perylene molecule is oriented at an angle β with respect to the C_∞ axis of the aggregate. In the LD experiments light propagates along the X axis and is either polarized along the Z or Y axes. In the emission anisotropy studies, the Z-polarized excitation light propagates along the X axis and the Z- and X-polarized emission is detected along the Y axis.

Corrections for a very low or negligible emission background of the solvents, micelles, and liquid crystals are within the experimental errors. Data were analyzed with a MINC-11/03 computer using the deconvolution software (DECAY V3.0a, ATROPY V1.0) developed by P.R.A. The steady-state fluorescence was recorded with a SPEX Fluorolog 112 spectrometer (SPEX Industries, Inc., Metuchen, NJ). LD spectra were measured with a home-built spectrometer described elsewhere,[15] and the absorption spectra were recorded on a Cary 219 (Varian, USA) spectrometer. The samples were thermostated within ±1 K.

General Considerations

Some liquid crystals align spontaneously or in an external electric or magnetic field and form macroscopically anisotropic systems of uniaxial symmetry. A schematic illustration of a macroscopically aligned detergent aggregate with a solubilized probe molecule is shown in Figure 1. The aggregate is oriented with its symmetry axis coinciding with the Z axis of a laboratory frame which also defines the symmetry axis and the optic axis of the system. Light propagating along the X axis with its linear polarization either along the Z or the Y axes is absorbed differently owing to the anisotropic orientation of the chromophores. This differential absorption defines the linear dichroism:

$$\mathrm{LD} \equiv A_Z - A_Y \qquad (1)$$

The orientation of the chromophores is characterized by an order parameter, S_g, that describes the average orientation of the absorption transition dipole moments with respect to the optical or Z axis of the sample. If the *ground-state orientational distribution* is denoted by $f_g(\beta)$, the order parameter is given by[7]

$$S_g = \int_0^\pi \tfrac{1}{2}(3\cos^2\beta - 1)\, f_g(\beta) \sin\beta \, d\beta \qquad (2)$$

where β stands for the angle between the transition dipole moment and the Z axis. S_g can be calculated[7,15] from LD and absorption spectra according to

(15) Johansson, L. B.-Å.; Davidsson, Å. *J. Chem. Soc., Faraday Trans. 1* **1985**, *81*, 1373.

$$LD/A_Y = 3S_g/(1 - S_g) \quad (3)$$

In a fluorescence experiment where the incident excitation light propagates along the X axis and is polarized along the Z axis (cf. Figure 1) we monitor the intensities emitted along the Y axis and polarized along the Z and X axes. These are denoted by $F_{zz}(t)$ and $F_{zx}(t)$, respectively, and they define the emission anisotropy, $r(t)$ according to:

$$r(t) = [F_{zz}(t) - F_{zx}(t)]/[F_{zz}(t) + 2F_{zx}(t)] \quad (4)$$

It has been shown[16-21] that generally the anisotropy could be separated as

$$r(t) = r_{dyn}(t) + r(t_\infty) \quad (5)$$

Different motions influencing the orientation of a fluorophore are described by $r_{dyn}(t)$. The static anisotropy, $r(t_\infty)$ is a limiting plateau value obtained a time $t = t_\infty$ after excitation. $r(t_\infty)$ represents the anisotropy of an *equilibrium orientational distribution* ($f_e(\beta)$) *of excited fluorophores*. Alternatively, $r(t_\infty)$ can be considered as the anisotropy of a macroscopically oriented distribution of fluorophores that has been excited without introducing any photoselection (i.e., isotropic excitation). For a macroscopically uniaxial system[7,21]

$$r(t_\infty) = \int_0^\pi \tfrac{1}{2}(3\cos^2\beta - 1) f_e(\beta) \sin\beta \, d\beta \equiv S_e \quad (6)$$

Thus, the order parameter, S_e, contains information about the orientation of the *emission* transition dipole moment. Different models describing $r_{dyn}(t)$ are available but often a phenomenological description is used:

$$r_{dyn}(t) = \beta_1 \exp(-t/\gamma_1) + \beta_2 \exp(-t/\gamma_2) \quad (7)$$

γ_1 and γ_2 are correlation times of the various motions that effect the orientation of the fluorophores and β_1 and β_2 are parameters.

A solution of fluorophores in a liquid solvent is mascroscopically isotropic and can, in contrast to a micellar solution, be considered as microscopically isotropic. For a solution, $r(t_\infty) = 0$ and $r(t)$ depend only on the rotations of the chromophore and the mutual directions of the molecule's fixed absorption and the emission dipole moments. By cooling a solution it is possible to eliminate the influence of the rotational diffusion. Measurements of $r(t)$ then yield information about the angle (θ) between the absorption and emission dipoles from

$$r(t) = \frac{2}{5}\frac{3\cos^2\theta - 1}{2} \quad (8)$$

If the transition dipole moments are parallel, $r = {}^2/_5$.

Micellar and cubic phases have properties in common with both a macroscopically anisotropic liquid crystal and a liquid solution. The local environment of a solubilized probe molecule is microscopically anisotropic and similar to that in a liquid crystal. Secondly, the orientational distribution of the aggregates in micellar and cubic phases is macroscopically isotropic which renders a similarity to the molecules of a liquid solution. Consequently, the fluorescence anisotropy of solubilized molecules in these microscopically anisotropic but macroscopically isotropic systems must include both static and dynamic molecular properties. The local anisotropic orientational distribution in an amphiphilic aggregate yields a static contribution while the dynamics include different motions that directly or indirectly cause a rotation of the excited molecule. There is a, presumably fast, local rotational motion of the fluorophore which we characterize by rotational correlation times denoted by ϕ_i. A slower translational motion of the probes within the aggregate as well as the overall rotational motion of the aggregate could contribute to $r(t)$. The correlation times Φ_{trans} and Φ_{rot} refer to these motions. Provided that the fluorescence lifetime is short compared to Φ_{trans} and Φ_{rot}, it may be shown that[16-21]

$$r(t) = {}^2/_5(1 - S^2) \sum_i \exp(-t/\phi_i) + {}^2/_5 S^2 \quad (9)$$

S ($=S_e = S_g$) describes the local orientation of the transition dipoles with respect to a surface normal of the aggregate. A more general treatment also includes the slow motions (Φ_{trans} and Φ_{rot}). Provided that these motions can be assumed to be independent of the fast local motions, one obtains[18,20]

$$r(t) = {}^1/_{10}[(1 - S^2) \sum_i \exp(-t/\phi_i) + S^2][3\exp(-t/\Gamma) + 1] \quad (10)$$

This equation models the fluorescence anisotropy of the probe molecules when solubilized in *cylindrical* aggregates. The correlation time Γ includes both the rotational motion about the C_∞ axis (Φ_{rot}) of the aggregate and the translational motion of the fluorophore about the C_∞ axis (Φ_{trans})

$$\frac{1}{\Gamma} = \frac{1}{\Phi_{rot}} + \frac{1}{\Phi_{trans}} \quad (11)$$

Results and Discussion

Spectra and Photophysics. The electronic *spectral* and *photophysical properties* of perylene (Pe), 2,5,8,11-tetra-*tert*-butylperylene (TBPe), methyl 4-(3-perylenyl)butyrate (PeBM), methyl 3-(3-perylenoyl)propionate (PPM), 3-(3-perylenoyl)-propionic acid (PPA), 9-(3-perylenoyl)nonanoic acid (PNA), and *N*-[9-(3-perylenoyl)nonanoyl]sphingosine-1-phosphocholine (PSM) have been investigated by absorption and fluorescence techniques. The structure formulas of these compounds are given in Figure 2. The fluorophores were dissolved in different solvents and solubilized in micelles and lyotropic liquid crystals. Both the absorption and the fluorescence spectra of the perylenyl derivatives, on one hand, and the perylenoyls, on the other, are significantly different. The vibronic structure of the absorption and fluorescence bands of TBPe and PeBM is very similar to that of perylene. The corresponding spectra of the perylenoyl compounds do not show any vibronic structure and are also more red-shifted. For all the fluorophores studied here, except from PSM in glycerol (vide infra), only minor shifts in the absorption spectra are observed between different host media. However, the fluorescence spectra of the perylenoyl molecules show both a strong red shift and broadening upon increasing polarity of the medium which is not found for the perylenyls. In the viscous solvents glycerol and 1,2-propanediol the fluorescence spectra of the perylenoyl compounds are markedly red-shifted with increasing temperature. This is illustrated in Figure 3A which shows the spectra of PNA in 1,2-propanediol at 209 and 298 K. The maximum of the fluorescence band is red-shifted about 50 nm upon increasing the temperature, while the absorption band shows a blue shift of about 5 nm. The temperature dependence of the absorption spectrum of PSM in glycerol was unique among the systems studied. When this system is cooled from about 320 to 290 K, the absorption spectrum broadens and a peak appears at 428 nm as shown in Figure 4. These spectral changes correlate with a decreasing fluorescence intensity and a red-shifted fluorescence spectrum with increasing temperature. The red shift is very similar to that found for PNA and PSM in 1,2-propanediol. Time-resolved single photon counting experiments with PSM show that the photophysics can be fitted to a monoexponential decay with the fluorescence lifetime $\tau = 5.6$ ns at temperatures higher than ~320 K. At lower temperatures a sum of two or more exponential functions is needed. One of these lifetimes is about 5.6 ns, which is close to the lifetime of PPM, PNA, and PSM in 1,2-propanediol (cf. Table I). A probable explanation of the anomalous behavior of PSM in glycerol is an aggregation of PSM molecules similar to the formation of lipid aggregates in water and/or glycerol solutions.[22-24] In

(16) Jähnig, F. *Proc. Natl. Acad. Sci. U.S.A.* **1979**, *76*, 6361.
(17) Zannoni, C.; Arcioni, A.; Cavatorta, P. *Chem. Phys. Lipids* **1983**, *32*, 179.
(18) Szabo, A. *J. Chem. Phys.* **1984**, *81*, 150.
(19) Van der Meer, B. W.; Kooyman, R. P. H.; Levine, Y. K. *Chem. Phys.* **1982**, *66*, 39.
(20) Eriksson, P.-O.; Johansson, L. B.-Å.; Lindblom, G. In *Surfactants in Solution*, Mittal, K. L., Lindman, B., Eds.; Plenum: 1984; Vol. 1.
(21) Fisz, J. J. *Chem. Phys.* **1985**, *99*, 177.
(22) Tanford, C. *The Hydrophobic Effect*; Wiley-Interscience: New York, 1980.

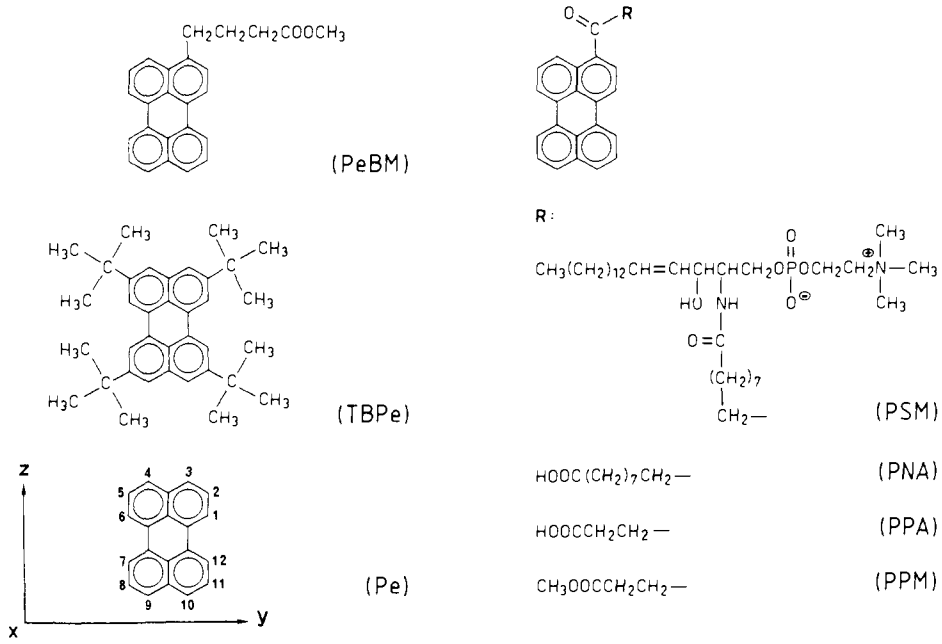

Figure 2. Structure formulas of methyl 4-(3-perylenyl)butyrate (PeBM), 2,5,8,11-butylperylene (TBPe), perylene (Pe), *N*-[9- (3-perylenoyl)nonanoyl]sphingosine-1-phosphocholine (PSM), 9-(3-perylenoyl)nonanoic acid (PNA), 3-(3-perylenoyl)propionic acid (PPA), methyl 3-(3-perylenoyl)-propionate (PPM). The *y* and *z* axes of a coordinate system are fixed in the plane of the perylene molecule so that the $S_0 \rightarrow S_1$ transition dipole moment coincides with the *z* axis.

these aggregates the chromophore–chromophore distances may be short which would govern strong electronic interactions such as exciton coupling between the chromophores. According to the theory of exciton coupling,[25,26] either a red- or a blue-shifted band appears relative to the monomer spectrum depending on the mutual orientation of the interacting chromophores. The blue-shifted band at 428 nm may be caused by coupling between perylenoyl molecules whose transition dipoles are mutually parallel. The complicated photophysics observed at lower temperatures could furthermore be due to energy transfer between excited monomers and aggregates of perylenoyl molecules.

Time-resolved fluorescence experiments show that the photophysics of the perylenyl and the perylenoyl compounds in solvents is monoexponential (cf. Table I). Taking PNA as an example, we conclude that the lifetimes are very similar, ranging between 5.0 and 5.7 ns and seem to increase slightly with increasing polarity of the solvent. The fluorescence emission of both the perylenoyl and the perylenyl compounds is quenched by O_2 as revealed by a comparison of the spectra obtained after bubbling the samples with N_2 and O_2. Such experiments show that the quantum yield in ethanol at 298 K decreases by a factor of about 2 for all the compounds. In the micellar and liquid crystalline system the photophysics of the perylenoyl derivatives is, contrary to that of the perylenyls, more complicated. In the lyotropic nematic liquid crystalline phase (LNLC) composed of potassium dodecanoate, KCl, and D_2O the fluorescence is dominated by a lifetime of 7 ns but a few percent of the intensity is due to a shorter lifetime of 1–4 ns for PNA or PSM. The presence of a biexponential or a more complex fluorescence decay is even more evident from the study of perylenoyls situated in micelles and a cubic liquid crystal of $C_{12}EO_5$ and water. Here, around 80% of the intensity corresponds to a lifetime of 7 ns while the remaining intensity is due to a lifetime of about 5 ns. Futhermore, the lifetimes depend on the emission wavelength. The fluorescence decay of, for example, PSM in the cubic phase of $C_{12}EO_5$ at 286 K is biexponential with the lifetimes 6.9 (80%) and 5.2 ns at 550 nm while one obtains 5.4 (85%) and 1.7 ns at 500 nm. However, the photophysics of methyl 4-(3-perylenyl)butyrate (PeBM) solubilized in the $C_{12}EO_5$–water system is found to be independent of the emission wavelength. The heterogeneity in fluorescence lifetimes and the anomalous red shift of the emission spectrum in polar media are only observed for the perylenoyl compounds. The main chemical difference between the perylenyl and the perylenoyl chromophores is the carbonyl group covalently bound to the perylene moiety. Thus the spectral and photophysical differences must originate from this group. A qualitative explanation to the heterogeneity observed is that the perylenoyl fluorophores are heterogenously distributed between regions of different polarity in the surfactant aggregate. This is furthermore supported by the anisotropy studies of PeBM and PNA solubilized in the cubic phase of $C_{12}EO_5$ at 281 K. As can be seen in Figure 3B both the excitation and emission anisotropy of PeBM are independent of the wavelength, but this is not the case for PNA. A deeper insight into this heterogenity would be gained by utilizing the recently developed decay-associated-spectra techniques.[33,34]

Polarization of Electronic Transitions. The *electronic absorption* ($S_0 \rightarrow S_1$) and *emission* ($S_0 \leftarrow S_1$) *transition dipole moments* of perylene are polarized[27-30] in the molecular plane along the *z* axis indicated in Figure 2. The absorption transition dipole has the same polarization along the whole vibronic progression in the region 350–450 nm which was also recently shown by linear dichroism (LD).[7] Here, LD of the various perylene and perylenoyl derivatives when solubilized in the LNLC phase has been measured. LD of the LNLC system, macroscopically and uniaxially aligned by a strong magnetic field, was determined with the electric field vector of light polarized parallel (Z) and perpendicular (Y) to the optic axis. The ratio $LD/A_Y \equiv (A_Z - A_Y)/A_Y$ was calculated for the perylenyl and the perylenoyl probes for the wavelengths regions 350–450 and 400–500 nm, respectively. In Figure 5 $LD(\lambda)/A_Y(\lambda)$ of PNA is displayed together with its absorption spectrum. The constant value of $LD(\lambda)/A_Y(\lambda)$ shows that the polarization of the electronic transition dipole in PNA does not depend on the excitation wavelength, and it furthermore suggests that this band corresponds to the $S_0 \rightarrow S_1$ transition. Similar

(23) McDaniel, R. V.; McIntosh, T. J.; Simon, S. A. *Biochem. Biophys. Acta* **1983**, *731*, 97.
(24) Larsen, D. W.; Rananavare, S. B.; Strary, F. E.; ElNokaly, M.; Friberg, S. E. *J. Phys. Chem.* **1984**, *88*, 4015.
(25) Kasha, M. *Radiation Res.* **1963**, *20*, 55.
(26) Cantor, C. R.; Schimmel, P. R. *Biophysical Chemistry I* W. H. Freeman: San Francisco, 1980.
(27) Tanaka, J. *Bull. Chem. Soc. Jpn.* **1963**, *36*, 1237.
(28) Shinitzky, M.; Dianoux, S. C.; Gilter, C.; Weber, G. *Biochemistry* **1971**, *10*, 2106.
(29) Zinsli, P. E. *Chem. Phys.* **1977**, *20*, 299.
(30) Pantke, E. R.; Labhart, H. *Chem. Phys. Lett.* **1973**, *23*, 476.

Table I. Fluorescence Lifetimes of Different Perylenyl and Perylenoyl Probes Dissolved in Solvents, Micelles, and Lyotropic Liquid Crystalline Phases, Measured by the Single Photon Counting Technique

fluorophore	medium	fluorescence lifetimes (ns) τ_1	τ_2	temp (K)
perylene (Pe)	ethanol (degassed)	5.2		
	ethanol	4.3		298
	1,2-propanediol	4.7		298
	glycerol	4.6		298
	LNLC	5.5		294
2,5,8,11-tetra-*tert*-butylperylene (TBPe)	ethanol	4.5		298
	1,2-propanediol	4.8		294
	LNLC	5.2		298
methyl 4-(3-perlenyl) butyrate (PeBM)	ethanol	4.1		294
	1,2-propanediol	4.6		294
	glycerol	4.4		298
	LNLC	5.1		294
	$C_{12}EO_5$	5.3		294
	(micelles)	5.3		286
	$C_{12}EO_5$ (cubic liq. phase)	5.0		286
methyl 3-(3-perylenoyl) propionate (PPM)	ethanol	5.5		
	1,2-propanediol	5.8		294
	LNLC	6.9		298
9-(3-perylenoyl) nonanoic acid (PNA)	ethanol (degassed)	6.3		
	ethanol	5.4		298
	methanol (CH_3OH)	5.5		294
	methanol (CH_3OD)	5.4		294
	dioxane	5.1		294
	olive oil	5.0		294
	1,2-propanediol (degassed)	5.8		294
	1,2-propanediol	5.7		294
	LNLC	7.0 (>95%)	3 ± 1	293
9-(3-perylenoyl) nonanoic acid	$C_{12}EO_5$ (micelles)	6.9 (≈80%)	5.8	295
	$C_{12}EO_5$ (cubic (liq. phase)	6.9 (≈80%)	5.1	277
N-[9-(3-perylenoyl) nonanoyl]sphingosine-1-phosphocholine (PSM)	ethanol	5.5		298
	1,2-propanediol	5.8		294
	glycerol	5.6		333
	LNLC	6.9 (>98%)	1 ± 0.5	293
	$C_{12}EO_5$	7.0 (≈80%)	4.8	293
	(micelles)	7.0 (≈70%)	5.6	286
	$C_{12}EO_5$ (cubic liq. phase)	6.9 (≈80%)	5.2	286

[a] The compositions of the micellar, the cubic liquid crystalline phases of $C_{12}EO_5$, and water and the lyotropic nematic liquid crystal (LNLC) are given in the Materials section.

results were obtained and the same conclusion was drawn for all fluorophores except for TBPe which did not show any LD (vide infra).

The fluorescence excitation anisotropy contains the same information as an LD experiment with the benefit of not requiring a macroscopically aligned sample. The excitation anisotropy of all fluorophores has been determined for solutions of 1,2-propanediol and, when soluble, also in glycerol. Typical excitation spectra and anisotropy data are shown in Figure 3A which are obtained for PNA in 1,2-propanediol. The anisotropy measured at 209 and 298 K is independent of the excitation wavelength. This fact alone confirms the conclusion already drawn from the LD studies, that the electronic absorption transition dipole has one well-defined direction in the wavelength region 400–500 nm. Taken together, the excitation anisotropy reveals only one dipole moment for the $S_0 \rightarrow S_1$ transition of the different fluorophores in this study.

Generally, the emission anisotropy yields information concerning the angle between the absorption and emission transition dipole moments which is most easily extracted if the fluorophores undergo a negligible rotational motion during their fluorescence lifetime. A measurement at 209 K of PNA in 1,2-propanediol fullfills this requirement and the emission anisotropy obtained is displayed in Figure 3A. The anisotropy is constant over the emission band, and a value of 0.38 is found which is close to the value previously reported[28] for perylene in 1,2-propanediol at 223 K. The maximum theoretical value is 2/5, which is expected for parallel absorption and emission dipoles. Our value is only slightly smaller and therefore strongly suggests that the transition dipole moments in PNA are parallel. This is also found for the other perylenoyl compounds. We conclude that the absorption and the emission transition dipoles are parallel for all the perylenyl and perylenoyl compounds investigated here. This shows that the mutual orientation of their dipoles does not change when the symmetry of the perylene fluorophores is lowered from point group D_{2h} to C_s. However, it is not evident that the polarization of the dipoles is *along* the molecular z axis (indicated in Figure 2) for the fluorophores which belong to the C_s point group of symmetry.

Molecular Orientation in Ground and Excited States. The fluorescent probes studied here are easily solubilized in the aggregates of the lyotropic nematic liquid crystalline (LNLC) phase that easily aligns in a magnetic field. The rod-shaped aggregates[32] of amphiphiles as well as the solubilized molecules become thereby uniaxially oriented. From LD and time-resolved fluorescence anisotropy experiments on such a system, model independent information about the orientation of the chromophores can be extracted. LD and the limiting anisotropy ($r(t_\infty)$) yield, as is pointed out in General Considerations, the order parameter of the chromophore in its electronic ground (S_g) and excited (S_e) states, respectively. The time-dependent anisotropy ($r(t)$) of PNA in the LNLC phase is illustrated in Figure 6C and clearly shows that $r(t)$ rapidly becomes a constant with time. A numerical evaluation of the excited-state order parameter is made by deconvolution of the sum and difference curves shown in Figure 6, A and B. Table II summarizes the ground- and excited-state order parameters of perylene and the different perylenyl and perylenoyl derivatives. The negative valued order parameters indicate that the "long" molecular z axis (cf. Figure 2) is preferentially oriented parallel to the hydrocarbon chains of the amphiphiles. For perylene, TBPe, and PeBM the order parameter decreases in the order $|S|_{Pe} > |S|_{PeBM} > |S|_{TBPe}$. A possible explanation to this could

Table II. Summary of Linear Dichroism (LD), Steady-State (r_s), and Time-Resolved ($r(t_\infty)$) Anisotropy Data of Different Perylenyl and Perylenoyl Derivatives When Solubilized in a Macroscopically Aligned Lyotropic Nematic Phase at 293 ± 1 K

fluorophore	LD/A_Y	ground-state order parameter S_g	steady-state anisotropy r_s	limiting anisotropy $r(t_\infty)$	excited-state order parameter S_e
perylene (Pe)	−0.265 ± 0.005	−0.097 ± 0.002	−0.083 ± 0.002	−0.099 ± 0.003	−0.099 ± 0.002
2,5,8,11-tetra-*tert*-butylperylene (TBPe)	0.00	0.00	0.053 ± 0.003	0.00	0.00
methyl 4-(3-perylenyl)butyrate (PeBM)	−0.173 ± 0.006	−0.061 ± 0.002	−0.016 ± 0.003	−0.056 ± 0.003	−0.056 ± 0.003
methyl 3-(3-perylenoyl)propionate (PPM)	−0.194 ± 0.006	−0.069 ± 0.002	−0.050 ± 0.003	−0.112 ± 0.003	−0.112 ± 0.003
3-(3-perylenoyl)propionic acid (PPA)	−0.375 ± 0.006	−0.143 ± 0.002	−0.146 ± 0.003	−0.171 ± 0.003	−0.171 ± 0.003
9-(3-perylenoyl)nonanoic acid (PNA)	−0.307 ± 0.006	−0.114 ± 0.002	−0.050 ± 0.003	−0.114 ± 0.003	−0.114 ± 0.003
N-[9-(3-perylenoyl)nonanoyl]sphingosine-1-phosphocholine (PSM)	−0.222 ± 0.006	−0.079 ± 0.003	−0.001 ± 0.003	−0.081 ± 0.003	−0.081 ± 0.003

[a] Excitation and emission wavelengths were 410 and 450 nm for the perylene and the perylenyl derivatives. The corresponding wavelengths of the perylenoyl probes were 450 and 550 nm, respectively.

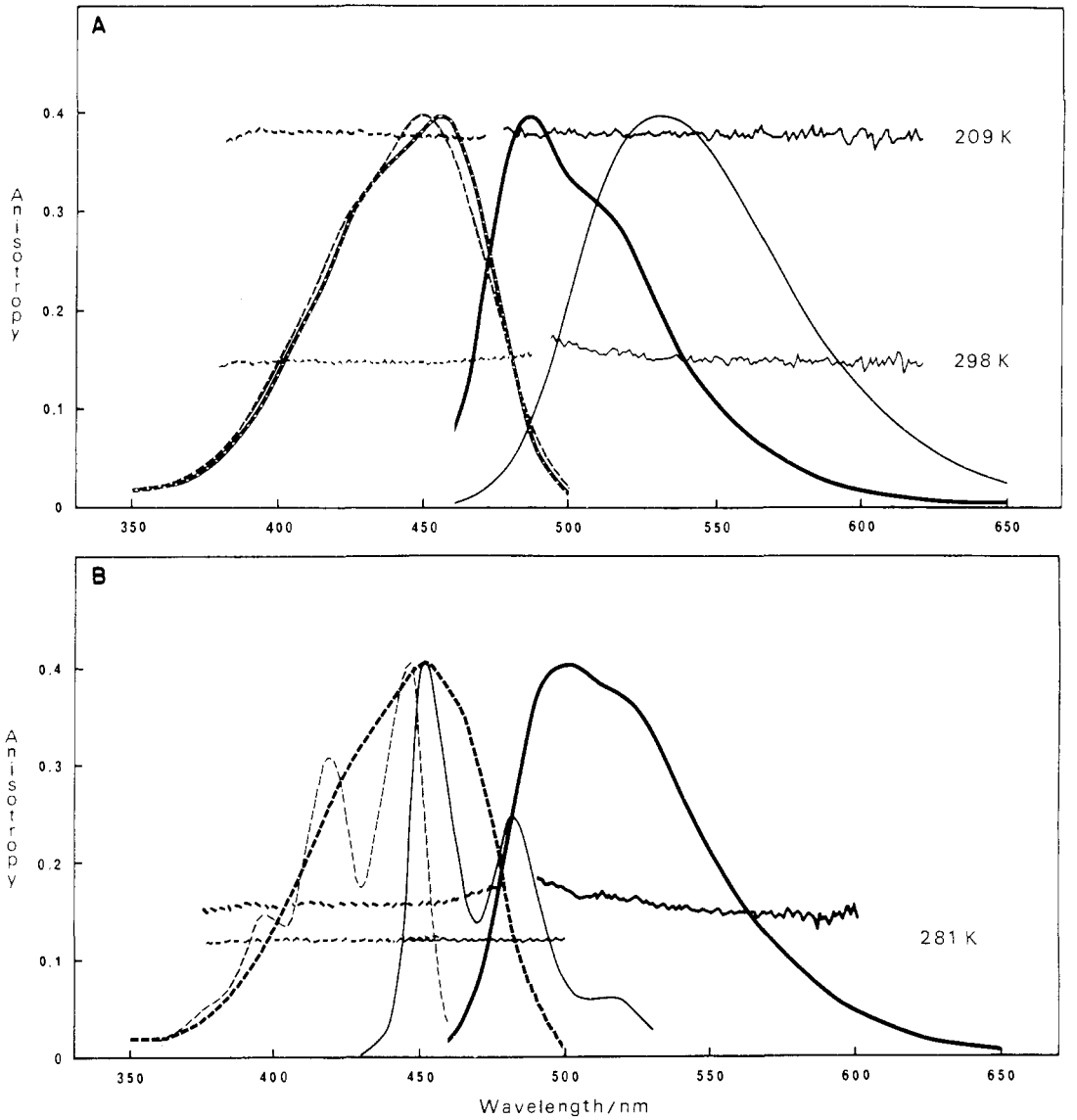

Figure 3. (A) Fluorescence excitation spectra and excitation anisotropy curves of 9-(3-perylenoyl)nonanoic acid (PNA) in 1,2-propanediol, at 209 and 298 K are displayed to the left. Fluorescence emission spectra and emission anisotropy curves at 209 and 298 K, when excited at 440 nm, are displayed to the right. (B) Fluorescence excitation and emission spectra (blue-shifted and showing vibronic structure) together with the excitation and emission anisotropies of methyl 4-(3-perylenyl)butyrate (PeBM) solubilized in the cubic phase of $C_{12}EO_5$ at 281 K. The red-shifted spectra and anisotropy curves are obtained for PNA in the corresponding cubic phase at 281 K.

be that PeBM and TBPe penetrate deeper toward the interior of the aggregate where the orientation of the alkyl segments is very low. This is expected since the hydrophobicity should decrease in the order TBPe > PeBM > Pe. The ground- and excited-state order parameters of these molecules are, as shown in Table II, very similar. This means that the orientational distribution is not significantly affected by the change in polarity upon excitation of the chromophores. S_g and S_e of PPM and PPA are significantly different and $|S_g| < |S_e|$. A qualitative explanation to this is that the polarity of these chromophores is higher in the excited state as is usually the situation.[31] These relatively small molecules would thereby redistribute in their excited state toward the polar water interface. Since the orientation of the hydrocarbon segments increases in this region, the order parameter, $|S_e|$, of a solubilized molecule would also increase. Neither PNA nor PSM changes its orientational distribution upon or after excitation although the same change in polarity as that of PPM and PPA is expected. One likely explanation may be that the chromophoric part of PNA and PSM is more rigidly anchored in the aggregate owing to the large nonanoic acid and sphingosine–phosphocholine moieties. These data suggest that PNA, PSM, and PeBM are the most suitable as lipid probes.

Motions of the Fluorophores. The fluorescence anisotropy of a probe molecule situated in a microscopically anisotropic environment, such as that of a micellar or liquid crystalline aggregate, contains information about both fluorophore orientation and motions. The steady-state and the time-resolved anisotropy ($r(t)$) of the different perylenyl and perylenoyl probes in the LNLC phase have been studied and the results are presented in Table III. The rod-shaped micellar aggregates of the LNLC phase align with their long axis mutually parallel and form a macroscopically uniaxial liquid crystal with an optical axis.[32] In the anisotropy experiments the excitation light was polarized parallel to the optic axis. This means that only the *local* rotational motion of the probe and the rotational motion of the C_∞ axis of the aggregate contribute to $r(t)$.[14] The latter kind of motion is slow.[14] Since a limiting anisotropy $r(t_\infty)$ is reached during the fluorescence decay

(31) Liptay, W. In *Excited States* Lim, E. C., Ed.; Academic Press: New York, 1974; Vol. 1.

(32) Johansson, L. B.-Å.; Söderman, O.; Fontell, K.; Lindblom, G. *J. Phys. Chem.* **1981**, *85*, 3694.

(33) Beechem, J. M.; Ameloot, M.; Brand, L. *Excited State Probes for Biochemistry & Biology*. Szabo, A., Massoti, L., Eds.; NATO ASI, Plenum: New York, 1985.

(34) Löfroth, J.-E. *J. Phys. Chem.* **1986**, *90*, 1160.

Table III. Fluorescence Steady-State and Time-Resolved Fluorescence Anisotropy Data Obtained for the Different Perylenyl and Perylenoyl Derivatives Dissolved in the LNLC Phase, the Micellar and Cubic Liquid Crystalline Phases of $C_{12}EO_5$, and Water[a]

fluorophore	system	fluorescence anisotropy $r(t) = \sum_{i=1}^{2}\beta_i \exp(-t/\gamma_i) + r(t_\infty)$					steady-state anisotropy	temp
		β_1	γ_1 (ns)	β_2	γ_2 (ns)	$r(t_\infty)$	r_s	(K)
perylene (Pe)	LNLC	0.16	0.6 ± 0.2			−0.099 ± 0.002	−0.083 ± 0.003	293
2,5,8,11-tetra-*tert*-butylperylene (TBPe)	LNLC	0.30	1.2 ± 0.1			0.00	0.053 ± 0.003	293
methyl 3-(3-perylenyl)butyrate (PeBMe)	LNLC	0.29	0.8 ± 0.1			−0.056 ± 0.003	−0.016 ± 0.003	293
methyl 3-(3-perylenoyl)propionate (PPM)	LNLC	0.23	0.3 ± 0.2	0.18	3.2 ± 0.5	−0.112 ± 0.003	−0.050 ± 0.003	293
3-(3-perylenoyl)propionic acid (PPA)	LNLC	0.15	1.3 ± 0.3			−0.171 ± 0.003	−0.146 ± 0.003	293
9-(3-perylenoyl)nonanoic acid (PNA)	LNLC	0.17	0.6 ± 0.2	0.16	3.4 ± 0.6	−0.114 ± 0.003	−0.050 ± 0.003	293
N-[9-(3-perylenoyl)nonanoyl]sphingosine-1-phosphocholine (PSM)	LNLC	0.21	3.8 ± 0.5			−0.081 ± 0.003	−0.001 ± 0.003	293
PNA	$C_{12}EO_5/H_2O$ (micellar phase)	0.19	3.6 ± 0.3	0.11	20.0 ± 3	0.01	0.152 ± 0.003	275
		0.19	3.4 ± 0.3	0.11	18.0 ± 3	0.01	0.134 ± 0.003	280
		0.21	2.8 ± 0.2	0.06	17.3 ± 4	0.00	0.110 ± 0.003	286
		0.20	1.8 ± 0.2	0.05	9.3 ± 2	0.00	0.071 ± 0.003	298
	$C_{12}EO_5/H_2O$ (cubic phase)	0.20	3.92 ± 0.93	0.12	21.0 ± 3	0.01	0.162 ± 0.003	280
PSM	$C_{12}EO_5/H_2O$ (micellar phase)	0.20	3.6 ± 0.3	0.11	25.3 ± 4	0.02	0.156 ± 0.003	280
		0.21	3.6 ± 0.3	0.08	23.5 ± 6	0.01	0.132 ± 0.003	286
		0.21	2.2 ± 0.1	0.07	14.7 ± 2	0.01	0.096 ± 0.003	298
	$C_{12}EO_5H_2O$ (cubic phase)	0.20	5.4 ± 0.5	0.13	40 ± 10	0.02	0.196 ± 0.003	280
		0.21	3.1 ± 0.2	0.12	34 ± 4	0.01	0.165 ± 0.003	286

[a] Sample compositions are specified in the Materials section. Time-resolved fluorescence anisotropy data were fitted by deconvolution to the phenomenological equation $r(t) = \Sigma^2_{i=1}\beta_i \exp(-t/\gamma_i) + r(t_\infty)$. γ_i denotes correlation times, β_i are constants, and $r(t_\infty)$ is the limiting anisotropy reached at a time $t = t_\infty$ after excitation.

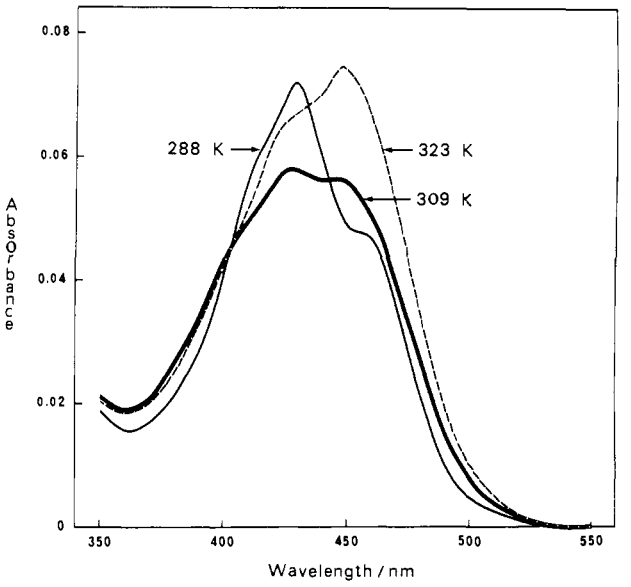

Figure 4. Absorption spectra of *N*-[9-(3-perylenoyl)nonanoyl]-sphingosine-1-phosphocholine (PSM) in glycerol recorded at 288, 309, and 323 K.

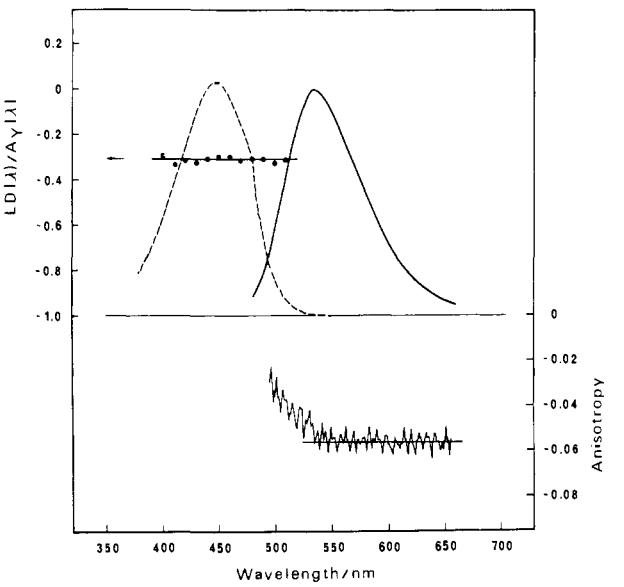

Figure 5. Absorption and fluorescence spectra of PNA solubilized in the macroscopically aligned LNLC phase at 293 K are shown in the upper half of the figure together with a plot of the reduced linear dichroism $LD(\lambda)/A_y(\lambda)$. The emission steady-state anisotropy recorded at the excitation wavelength 440 nm is shown in the lower part of the figure.

(cf. Figure 6C), this implies that a rotational motion of the C_∞ axis is negligible on the time scale of the present experiments. We therefore ascribe the correlation times (γ_1, γ_2) to the local rotational motions (ϕ_1, ϕ_2) of the fluorophore in the aggregates of the LNLC phase. The rotational rate ($1/\phi$) of the perylenyl probes decreases in the order $(1/\phi)_{Pe} > (1/\phi)_{PeBM} > (1/\phi)_{TBPe}$. This is in qualitative agreement with the diffusive rotational rate in solution that increases by the reciprocal volume of the rotating molecule (V_{mol}), i.e., $1/\phi \propto 1/V_{mol}$. Notice that the contribution of limiting anisotropy to $r(t)$ for TBPe is negligible. This indicates that TBPe is solubilized in the interior of the amphiphilic aggregate, where the local order is small and resembles that of a liquid. The vanishing LD also supports this interpretation. The rotational correlation times of the perylenoyl probes are significantly longer than those of the perylenyl molecules although, for example, PPM and PeBM have very similar van der Waals volumes. The PeCO moiety is more polar than the $PeCH_2$ moiety. Therefore, PPM is most likely localized closer to the water interface than PeBM, which will favor hydrogen bonding and thereby could reduce the rotational rate. In the LNLC phase PNA and PSM rotate most slowly (cf. Table III), which is compatible with the large substituents at the perylenoyl group.

The nonionic detergent $C_{12}EO_5$ and water form a micellar solution and a cubic liquid crystalline phase.[35] The cubic phase is optically isotropic, low-scattering, and extremly viscous (stiff), which makes it excellent in light spectroscopic studies. The structure of this phase is not known, but the detergents might be packed into cylindrical aggregates. The aggregates of the micellar phase are also most likely cylindrical. Here we have, utilizing PNA and PSM as reporter molecules, compared the fluorescence anisotropy, $r(t)$, of the micellar, the cubic, and the LNLC phases. This is, as far as we know, the first time-resolved fluorescence anisotropy study of a cubic lyotropic liquid crystal. The results, collected in Table III, show that the static contribution, $r(t_\infty)$, of $r(t)$ is small in the isotropic phases of $C_{12}EO_5$ compared with the

(35) Mitchell, D. J.; Tiddy, G. J. T.; Waring, L.; Bostok, T.; McDonald, M. P. *J. Chem. Soc., Faraday Trans. 1* **1983**, *79*, 975.

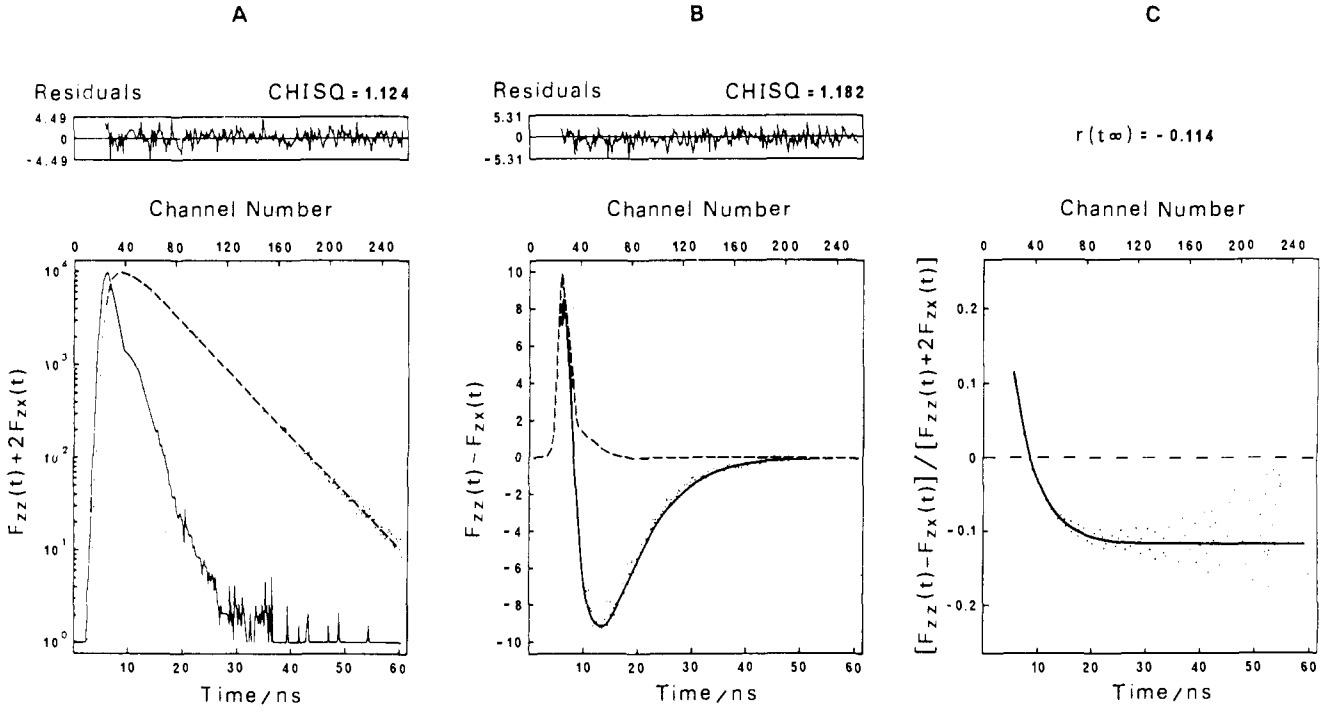

Figure 6. Time-resolved fluorescence data of PNA in the macroscopically aligned LNLC phase. (A) Decay of the photophysics (- - -) and the response function (—). (B) Difference curve from which the emission anisotropy $r(t) = 0.17 \exp(-t/0.6) + 0.16 \exp(-t/3.4)$ is calculated (—); response function (- - -). (C) Experimental and calculated decay curves of the emission anisotropy.

LNLC phase. However, the limiting anisotropy of solubilized fluorophores can be estimated. Consider rod-like aggregates of amphiphiles that are either macroscopically anisotropic, so that their long axis are mutually parallel, or macroscopically isotropic. For these systems $r(t_\infty)$ equals S_e and $^2/_5 S_g S_e$, respectively (cf. General Considerations). Since S_e and S_g are typically around 0.1, this explains the almost negligible static contribution of $r(t)$ for the micellar and cubic phases.

The rotational correlation times in the micellar and cubic phases are generally longer as compared to the LNLC phase. This can be explained by considering the different motions that may contribute to $r(t)$. These are the local rotational and the translational motions of the probes in the amphiphilic aggregates and the rotational motions of the aggregates (cf. General Considerations). We assume that the local motions are independent of the slower translational diffusion and the rotational diffusion of the aggregate. $r(t)$ for fluorophores situated in the micellar or cubic phases and the macroscopically anisotropic LNLC phase are then described by eq 10 and 5–7, respectively. Obviously, the slower motions contribute to $r(t)$ for the macroscopically isotropic systems. Provided that $\Gamma \gg \phi_i$, eq 10 may be rewritten as:

$$r(t) = {}^2/_5(1 - S^2)\sum_i \exp(-t/\phi_i) + {}^3/_{10}S^2 \exp(-t/\Gamma) + {}^1/_{10}S^2 \quad (12)$$

This equation predicts the experimentally determined $r(t)$ rather well. For a *local* order parameter (S) of 0.6 the preexponential factors $^2/_5(1 - S^2)$ and $^3/_{10}S^2$ are 0.26 and 0.11, respectively, while $r(t_\infty) = 0.036$. The first term of eq 12 could then be identified with the $\beta_1 \exp(-t/\gamma_1)$ term (cf. Table III). This implies that γ_1 is equal to the fast local rotational motion (ϕ). An identification of the second term with the experimental term, $\beta_2 \exp(-t/\gamma_2)$, yields the correlation time of the slower motions $\Gamma = \gamma_2$. The local rotational correlation times ϕ in the micellar and cubic phases are very similar to those in the LNLC phase. The rotational correlation time of a spherical micelle (Φ_{rot}) can be estimated from the Perrin equation.[36] Φ_{rot} is found to be around 100 ns if a radius corresponding to the length of an extended $C_{12}EO_5$ molecule is chosen. This implies that contributions to Γ from the rotation of a cylindrical detergent aggregates can be neglected. We therefore conclude, regarding eq 11, that the correlation times of 10 to 40 ns are due to the translational diffusion of PNA and PSM in the detergent aggregates. As can be seen in Table III, Φ_{trans} of PSM is slightly longer which is compatible with its bulkiness compared to PNA.

As a comparison, we have calculated Φ_{trans} of $C_{12}EO_5$ from the translation diffusion coefficient (D_{exp}) measured with NMR. In the cubic phase composed at $C_{12}EO_5$ and water $D_{exp} = 8.5 \times 10^{-12}$ m^2/s at 285 K.[40] We estimate the correlation time of translational diffusion from[20]

$$\Phi_{trans} = R^2/6D \quad (13)$$

where

$$D \approx 3D_{exp} \quad (14)$$

where R is the radius of the aggregate. A radius of 3.0 nm, which is the approximate length of an extended $C_{12}EO_5$ molecule, yields $\Phi_{trans} = 60$ ns. Thus, Φ_{trans} of the amphiphile $C_{12}EO_5$, PNA, and PSM are all of the same order of magnitude. This finding suggests that the translational motion of the lipids and that of the solubilized probe molecules might be cooperative. This deserves an extended examination since it may gain a deeper insight into the mechanism of lipid translational diffusion.

Acknowledgment. We are very grateful to Mrs. Eva Vikström for a skillful technical assistance, to Dr. Per-Olof Eriksson for the NMR measurements, and to Dr. T. A. Chibisova for a specimen of 4-(3-perylenyl)butyric acid.

(36) Cantor, C. R.; Schimmel, P. R. *Biophysical Chemistry II*, W. H. Freeman: San Francisco, 1980.
(37) Molotkovsky, J. G.; Bergelson, L. D. *Bioorg. Khim.* **1982**, *8*, 1256.
(38) Zinke, A.; Troger, H.; Ziegler, E. *Chem. Ber.* **1940**, *73*, 1042.
(39) Gaver, R. C.; Sweely, C. C. *J. Am. Oil Chem. Soc.* **1965**, *42*, 294.
(40) Eriksson, P.-O. Department of Physical Chemistry, University of Umeå, S-901 87 Umeå, Sweden, personal communication.